# GaAs-Based Metamorphic Technology

R. E. Leoni III, W. E. Hoke, C. S. Whelan, P. F. Marsh, P. C. Balas II, J. G. Hunt,
K. C. Hwang, S. M. Lardizabal, C. Laighton, S. J. Lichwala, Y. Zhang, and T. E. Kazior

Raytheon RF Components, 362 Lowell St., Andover, MA 01810
**Email:** rleoni@raytheon.com **Phone:** (978)-684-5311 **Fax:** (978)-684-5345

**Abstract**

**The past year has been an exciting one for metamorphic technology. With the capability of providing InP-based device performance on GaAs substrates, MMIC foundries are looking to this technology for a low cost alternative for wide bandwidth, low noise, high frequency and opto-electronic applications [1]. In particular, the increasing interest in high-speed devices for optical data links has fueled the growth of efforts in both InP and GaAs-based metamorphic technologies. In this paper, we will discuss the current status of metamorphic technology at Raytheon and our efforts to develop wide bandwidth / high data rate 1.55 µm opto-electronic components on GaAs.**

## INTRODUCTION

InP based devices have been the technology of choice for low noise, high frequency and broad bandwidth circuits due to their excellent carrier transport characteristics and carrier confinement. In addition, devices capable of absorbing 1.55 µm radiation may be fabricated on InP substrates. The high indium content InGaAs layers that provide these desirable characteristics are lattice-matched to InP but highly mismatched to GaAs substrates.

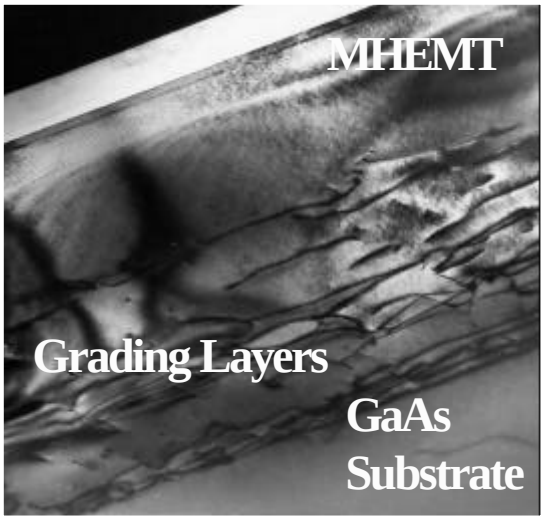


**Fig. 1:** TEM photograph of metamorphic HEMT material. While the buffer layers contains a large amount of defects, very few propagate into the active layer.

Recently, metamorphic buffer layer technology has been developed [2-5] which provides a method through which high indium content layers may be grown on GaAs. The metamorphic buffer absorbs the strain of lattice mismatch and prevents the vertical propagation of dislocations, thereby maintaining the quality of the device active layers (Fig. 1). In addition, metamorphic buffers allow the growth of practically any indium content layers, which is highly desirable for device optimization. Briefly, the metamorphic buffer layer is an approximately 1.5 µm AlGaInAs layer in which the indium concentration is linearly increased to expand the lattice constant from GaAs typically to that of InP. During the indium grading, the aluminum composition is approximately 40%, which results in good buffer layer resistivity for device isolation.

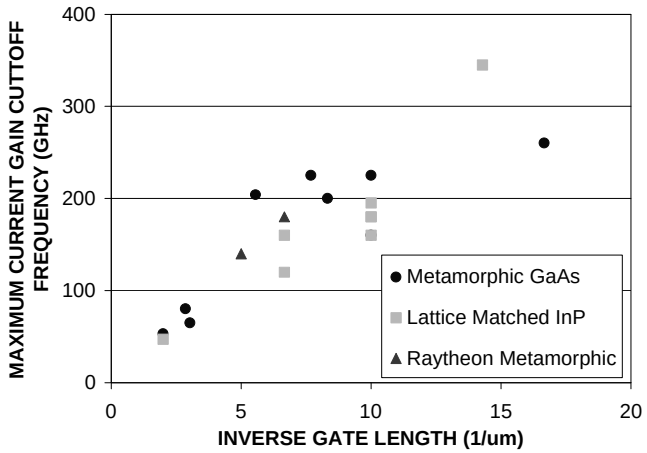


**Fig. 2:** Maximum current gain cutoff frequency ($F_T$) as a function of inverse gate length for reported InP and metamorphic GaAs HEMTs. [10, 23 – 37]

## METAMORPHIC HEMT

While some metamorphic HBT work has been reported [6, 7, 8], to date the majority of metamorphic transistor development has been in the area of HEMTs. Published device (Fig. 2) and amplifier [9] performance data have shown the InP and metamorphic HEMT (MHEMT) technologies to be equivalent. In fact, impressive results have been presented by IEMN on a 60 nm gate length MHEMT that provides an $F_T$ and $F_{MAX}$ of nearly 300 and 500 GHz respectively [10]. Besides performance, InP and metamorphic HEMTs have been shown to have equivalent levels of reliability [11, 12]. Figure 3 shows the results of accelerated life testing performed on Raytheon development and production foundry MHEMTs plotted with published results for other InP and metamorphic HEMTs. Mean-time-to-failures of greater than $10^6$ hours at 125 °C are obtained

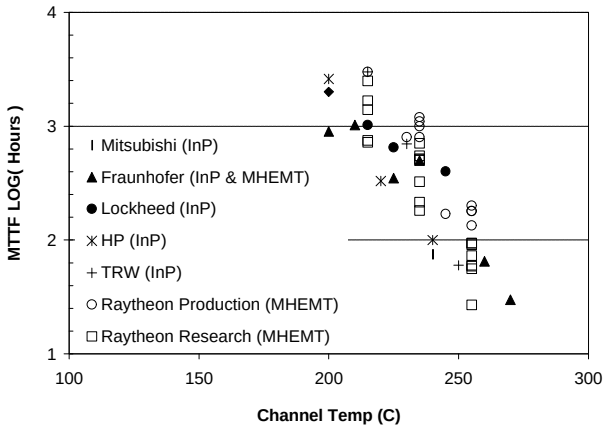


**Fig. 3:** Mean-time-to-failure of InP and metamorphic HEMTs [12, 37-41] at elevated temperatures and at low noise biases. Failure criteria range from 10% to 20% changes in Idss, Gm, or 1 dB drop in gain. Raytheon's Failure criteria are 10% reduction in Gm or 15% reduction of Idss.

for these technologies, which is adequate for space qualification.

Although the performance and reliability of InP and metamorphic HEMTs are equivalent, the costs associated with their production differ. For a 4" MHEMT structure, the less expensive GaAs substrate translates to a cost per wafer savings of nearly $1,000 (Fig. 4). Also, InP is potentially a lower- yielding technology due to its lower breakage strength.

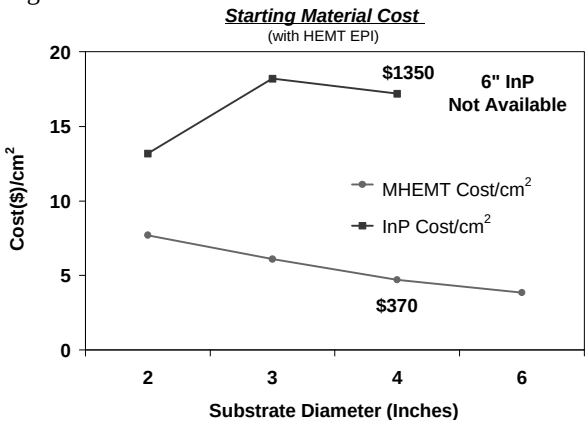


**Fig. 4:** The starting cost per square centimeter of a HEMT structure on GaAs is significantly lower than InP, providing significant financial incentive for pursuing metamorphic growth.

The Raytheon RF Component development line low noise MHEMT has a thick $In_{0.6}Ga_{0.4}As$ channel. During processing, a single wide recess is selectively etched in the material upon which a 0.15 µm length 'T' gate is placed. Due to the selective gate recess, pinch-off voltages are consistently –0.7 V. Typical peak transconductance and $I_{dss}$ for this process at a drain-source voltage of 1V are 850 mS/mm and 500 mA/mm respectively [13]. On-state and off-state breakdowns are 2.5 and 8V respectively. Biased at 1V and 90 mA/mm these devices show 0.24 dB $F_{min}$ with 16.2 dB associated gain at 12 GHz, and 0.61 dB $F_{min}$ with 13.8 dB $G_{assoc}$ at 26 GHz. Peak $F_T$ for this process is typically 180 GHz. Transfer of this process to the production line has been completed [14], The process is available as a foundry service.

A number of low noise and wide bandwidth amplifiers [15-17] have been demonstrated using this technology. The wide bandwidth traveling wave amplifier (TWA) [17] is of particular interest for high-speed data links up to 40 Gb/s. The amplifier consists of 6 cascode pair cells (Fig. 5) and uses purely resistive loads in order to extend the on chip low frequency range of operation. Figure 6 summarizes the s-parameters of 63 chips from a typical wafer. The amplifier has a high frequency 3 dB cutoff of approximately 45 GHz and a KHz range low frequency cutoff. Gain in a 50 Ω system is typically 16 dB with a 1.5 dB peak-to-valley variation to 40 GHz. RMS gain variation over this range is typically 0.25 dB. The chip is capable of providing over 3 dBm over the majority of the band, which is approximately 0.9V peak-to-peak in a 50 Ω system.

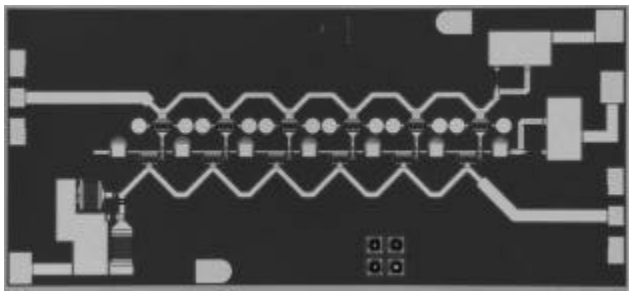

**Fig. 5:** Photograph of a dc – 45 GHz TWA. The amplifier consists of 6 cascode pair cells and occupies an area of 6.3 $mm^2$.

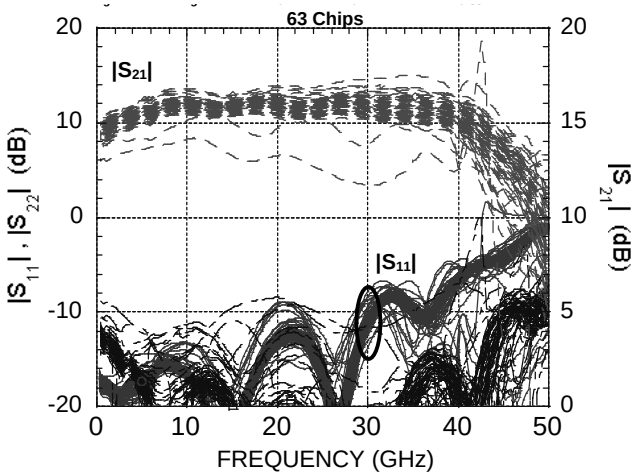


**Fig. 6:** S-parameters results of 63 MHEMT TWAs from a single wafer. The superimposed $S_{11}$, $S_{21}$, and $S_{22}$ of the amplifiers are displayed.

## METAMORPHIC PIN DIODES & PHOTORECEIVERS

In addition to transistors, top illuminated metamorphic PIN photodiodes which absorb in the 1.55 µm range have been reported [8, 18, 19]. Raytheon's PIN photiodiode consists of $In_{0.53}Ga_{0.47}As$ P+ anode and thick undoped drift layers grown on top of an N+ $In_{0.52}Al_{0.48}As$ cathode layer. A

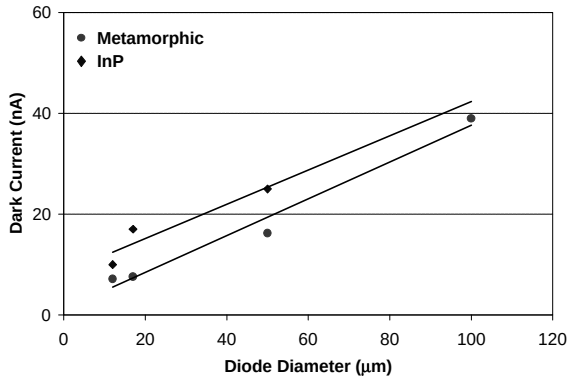


**Fig. 7:** The leakage current of metamorphic GaAs and InP 1.55 mm photodiodes exhibit approximately the same levels of dark current. Leakage current for both technologies shows an approximately linear dependence on device diameter, indicating little bulk leakage.

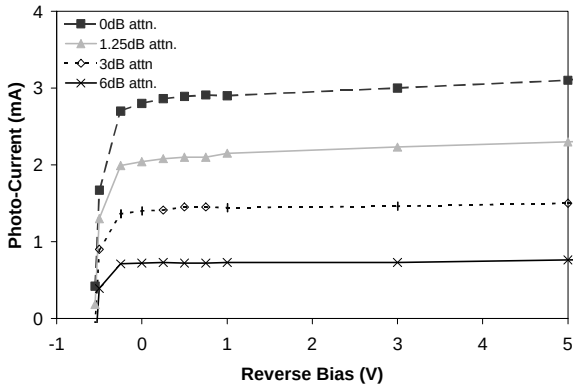


**Fig. 8:** Photocurrent as a function of optical power and reverse bias. The optical power is increased from 2.5 to 10 mW in 2.5 mW steps.

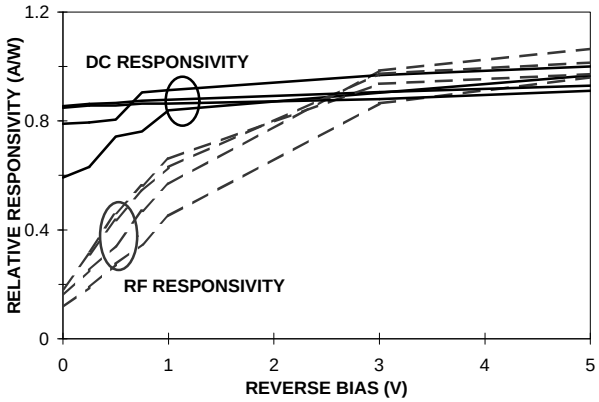


**Fig. 9:** Relative responsivity of a 10 μm photodiode tested at dc (solid lines) and 20 GHz responsivity calculated from the power delivered to a 50 W load. RF results show that a minimum of 3 V reverse bias is necessary.

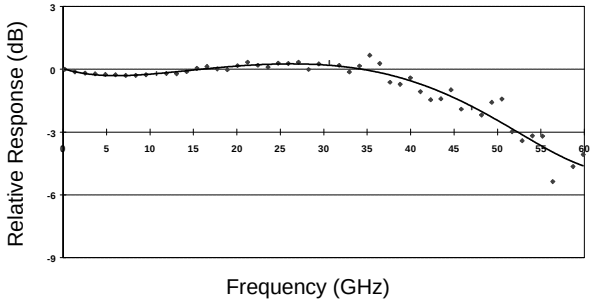


**Fig. 10:** Frequency response of a fixtured 10 μm metamorphic photodiode. The device provides greater than 50 GHz of bandwidth with a responsivity of 0.5 A/W.

metal stack consisting of Au/Ge is used for N+ contacts and a Ti/Pt/Au is deposited for P+ contacts. Air bridges are formed to connect the anode pad to the anode ring. Devices with optical diameters of 10, 20 … 50 μm in diameter are typically fabricated using this material.

The active layers in these structures are much thicker than those found in HEMTs and therefore are affected by residual strain in the buffer much more than the HEMTs. Any stress-induced dislocations that propagate into the device active layers will electrically show themselves as increased leakage current. Figure 7 displays typical leakage currents of both Raytheon's InP and metamorphic PIN photodiodes as a function of diode diameter. A quadratic dependence on diode diameter infers bulk-related leakage while a linear dependence indicates periphery-related leakage. Both technologies exhibit a roughly linear dependence on diameter and have about the same amount of dark current.

The metamorphic photodiodes have frequency responses and responsivities adequate for high data rate applications. Figure 8 shows the dc photocurrent for a 10 μm device. The data acquisition system used for this measurement has a 20 μm spot size and therefore is not capable of responsivity measurements. However, from the figure we see a linear relationship between current and optical power. From a comparison of relative dc responsivity and 20 GHz modulated light as a function of reverse bias, we see that the devices require at minimum 3 V reverse bias (Fig. 9). Fixtured 10 μm diameter metamorphic photodiodes biased at -5 V have greater than 50 GHz of bandwidth with 0.5 A/W responsivity (Fig. 10).

A photodiode and a wide bandwidth amplifier make up the front end of a photoreceiver. Using our TWA and InP photodiodes we have been able to build optical receivers for both analog and digital oriented applications. The frequency response of a 2-18 GHz receiver is shown in Figure 11. The module has an average responsivity of 90 V/W with a variation of +/- 15 V/W over its operational frequency and temperature ranges. Also, a hybrid photoreceiver with a 3 dB cutoff of 32 GHz has been demonstrated (Fig. 12). This is suitable for 40 Gb/s NRZ SONNET networks.

The interface between the a photodiode and wide bandwidth gain stage greatly affects the overall frequency response of a photoreceiver due to the high degree of mismatch between the photodiode, which electrically is a capacitively loaded current source, and amplifier. Therefore, for high data rate optical links there are great benefits to monolithic integration of photodiode and amplifier. With the ability to grow high indium content active layers on GaAs,

Raytheon and others are working towards the development of monolithically integrated metamorphic opto-electronic integrated circuits [20].

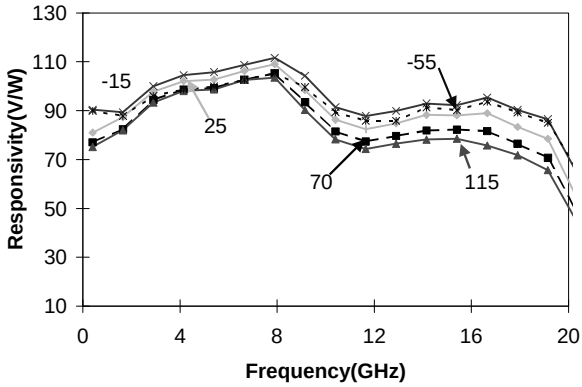


**Fig. 11:** Frequency response of a hybrid photoreceiver covering the majority of the frequency range up to 20 GHz. The receiver operates with little gain variation from –55 to 115°C.

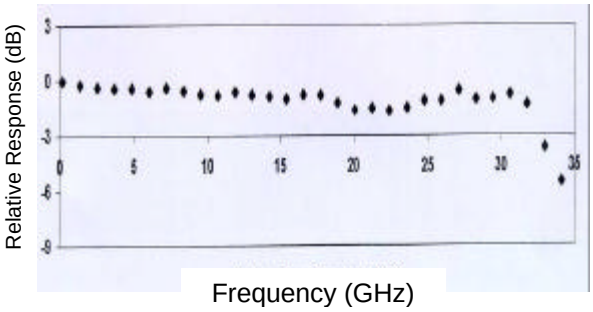


**Fig. 12:** Frequency response of a hybrid photoreceiver composed of a metamorphic TWA and InP photodiode.

## CONCLUSION

Metamorphic technology has been demonstrated to provide material with InP-like performance that can be processed at GaAs levels of manufacturability and cost. Ideally, all devices that can be produced on InP substrates may now be fabricated on GaAs. To date this has been shown to be true for HEMTs, HBTs, and photodiodes. Metamorphic technology also opens up the possibility of tailoring lattice constant for particular applications (eg. gain, noise figure, power, absorption, etc.) [21, 22] without having to contend with the issue of substrate induced strain and dislocations.

## ACKNOWLEDGEMENT

The authors would like to thank A. M. Joshi and X. Wang of Discovery Semiconductor for their help in assembling and testing the wide bandwidth photoreceivers.

## REFERENCES

[1] "Raytheon, OMMIC launch new MHEMT processes," *Compound Semiconductor*, page 11, Oct. 2001.
[2] W.E. Hoke, et al., *J. of Vacuum Science and Tech. B* 17, p. 1131 (1999).
[3] D. Lubyshev, et al., *J. of Vacuum Science and Tech., B* 19, p. 1510, 2001.
[4] M. Chertouk et al, *IEEE Electron Device Letters*, vol. 17, no. 6, pp. 273-275, 1996.
[5] M. Kawano et al, *IEEE Microwave and Guided Wave Letters*, Vol. 7, No. 1, pp. 6-8, 1997.
[6] S. Halder, et al., *Proc. of 2001 International Microwave Symp.*, p. 1885.
[7] W. K. Liu, *2001 InP and Related Materials Conf. Proc.*, p. 284.
[8] W.E. Hoke, et al., *J. of Vacuum Science and Tech., B* 19, p. 1505, 2001.
[9] P.M. Smith, et al., *Proc. of 2001 GaAs IC Symp.*, p. 7.
[10] A. Cappy, et al., *InP and Related Materials Conf. Proc.*, p. 192.
[11] P.F. Marsh et al., *Proc. of 2001 GaAs REL Workshop*, p. 119.
[12] M. Chertouk, et al., *2000 GaAs MANTECH Conf. Proc.*, p. 233.
[13] C.S. Whelan, et al, *2000 InP and Related Materials Conf. Proc.*, p. 337.
[14] C.S. Whelan, et al., *2001 CS-MAX Conf. Proc.*
[15] C.S. Whelan, et al., *IEEE J. Solid State Circuits*, Vol. 35, No. 9, 2000, pp. 1307-1311.
[16] P.F. Marsh, et al., *Proc. of 1999 International Microwave Symp.*, p. 105.
[17] R.E. Leoni III, et al., *Proc. of 2001 GaAs IC Symp.*, p. 133.
[18] C.S. Whelan, et al., *Proc. of 2001 GaAs IC Symp..*, p. 251.
[19] J.H. Jang, et al., *Electronics Letters*, Vol. 37, No. 11, pp. 707-708.
[20] Discovery Semiconductor Inc. "OEIC's: reality or laboratory curiosity?", results presented at *Panel Session 4 of the 2001 GaAs IC Symp.*
[21] C. S. Whelan, et al., *2000 InP and Related Materials Conf. Proc.*
[22] A. Cappy, et al., *Proc. of 1999 GaAs IC Symp.*, p. 217.
[23] D.C. Dumka, et al., *Electronics Letters*, Vol. 35, No. 21, pp. 1854-1855.
[24] D.C. Dumka, et al., *Device Research Conference Proc.*, pp. 83, 84.
[25] D.C. Dumka, et al., *IEEE Electron Device Letters*, Vol. 22, No. 8, pp. 364-366.
[26] D.L. Edgar, et al., *Electronics Letters*, Vol. 35, No. 13, pp. 1114-1115.
[27] M. Zaknoune, et al., *Electronics Letters*, Vol. 35, No. 19, pp. 1670-1671.
[28] F. Benkhelifa, et al., *InP and Related Materials 2000.* p. 290.
[29] R. Schmidt, et al., *Proc. of 2000 Symp. On High Performance Electron Devices for Microwave and Optoelectronic App.*, p. 95.
[30] K.C. Hwang, et al., *IEEE Electron Device Letters*, Vol. 20 No. 11, pp. 551-553.
[31] P. M. Smith, et al., *IEEE Microwave Guided Wave Letters*, Vol. 5, No. 7, pp. 230-232.
[32] S. Kimura, et al., *Proc. of 1999 Symp. On Circuits and Systems*, p. 488.
[33] K. Takahata, et al., *IEEE J. of Selected Topics in Quantum Electronics*, Vol. 6, No. 1, pp. 31-37.
[34] M. Boudrissa, et al., *IEEE Electron Device Letters*, Vol. 22, No. 6, pp. 257-259.
[35] H. Shigematsu, et al., *IEEE J. of Solid-State Circuits*, Vol. 36, No. 9, pp. 1309-1313.
[36] R. Lai, et al., *Proc. 2000 Electron Devices Meeting*, p. 175.
[37] Y.C. Chou, *Proc. of 2001 GaAs IC Symp.*, p. 174.
[38] N. Hayafuji, et al., *J. of the Electrochemical Soc.*, Vol. 145, No. 8, p. 2051.
[39] M. Chertouk, et al., *Proc. of 1999 GaAs ManTech Conf.*, p. 25.
[40] P.M. Smith, *Proc. of 1995 Military Communications Conf.*, p. 731.
[41] A. Wakita, et al., *Japanese J. of Applied Physics*, Vol. 38, pt. 1, No. 2B, pp. 1186-1188.